
Article:
Simoni, M., Hanein, T. orcid.org/0000-0002-3009-703X, Duvallet, T.Y. et al. (3 more authors) (2021) Producing cement clinker assemblages in the system : CaO-SiO2-Al2O3-SO3-CaCl2-MgO. Cement and Concrete Research, 144. 106418. ISSN 0008-8846

https://doi.org/10.1016/j.cemconres.2021.106418

Producing cement clinker assemblages in the system: $CaO-SiO_2-Al_2O_3-SO_3-CaCl_2-MgO$

Marco Simoni[1], Theodore Hanein[1]*, Tristana Y. Duvallet[2], Robert B. Jewell[2], John L. Provis[1], and Hajime Kinoshita[1]

[1] *University of Sheffield, Department of Materials Science & Engineering, S1 3JD, Sheffield, United Kingdom*
[2] *University of Kentucky Center for Applied Energy Research (UK-CAER), 2540 Research Park Drive, Lexington, KY, 40511, USA*
** Corresponding author: t.hanein@sheffield.ac.uk*

Abstract

The cement industry is carbon-intensive, and the valorisation of industrial side-streams/residuals for use as alternative raw materials can enable the cement industry to reduce its carbon footprint as well as promote resource efficiency. Apart from key clinker ingredients such as CaO, Al_2O_3, and SiO_2, industrial residues can also contain MgO, $CaCl_2$, and SO_3. Therefore, this study investigates the formation of cement clinker assemblages in the system $CaO-SiO_2-Al_2O_3-SO_3-CaCl_2-MgO$ at temperatures ranging between 1100 – 1300°C. The production of a clinker composed mainly of alinite and ye'elimite is first attempted; it is found that these phases cannot be simultaneously produced. Ternesite is also not compatible with alinite under the conditions studied. Wadalite is compatible with both ye'elimite and ternesite, while ternesite is also compatible with chlormayenite at 1150°C. Additionally, the low-temperature formation of alite was also observed with the presence of $CaCl_2$ in the raw-material mix.

Keywords: cement clinker production; alinite; ye'elimite; ternesite; calcium chloride; industrial circular economy; low-CO_2.

Highlights

- Alinite formation conditions are optimised
- Ye'elimite and alinite cannot be simultaneously produced
- Ternesite and chlormayenite are compatible at 1150°C
- Alite is formed at a reduced temperature of 1300°C
- Wadalite and chlorellestadite can incorporate chloride in cement clinker assemblages

1. Introduction

1.1. Background

Given the important environmental burden linked to cement manufacture [1], the industry is prioritising the search for low-carbon solutions. Among others, the valorisation of industrial side-streams for use as alternative raw materials and the manufacture of low-impact clinker, are major solutions. Side-streams from industries such as waste-to-energy plants [2, 3] and soda ash manufacture [4] contain CaO-SiO_2-Al_2O_3 in varying quantities, and can be attractive alternative raw materials for the manufacture of cement clinker as they would reduce the use of CO_2-containing limestone. However, they also comprise significant amounts of $CaCl_2$, MgO, and SO_3 [5, 6] in quantities which are unusual for conventional cement kiln raw-meal. Chloride is usually avoided in cements as it can exacerbate the corrosion of mild steel reinforcement in concrete [7]; however, Cl-containing cement clinker can still be employed where steel reinforcement is not utilised or where the Cl is not labile. In addition, more than 60% of cement usage is unreinforced [8]. To enhance industrial circular economy and decarbonisation, it is advantageous to understand clinker phase assemblages in the system: CaO-SiO_2-Al_2O_3-SO_3-$CaCl_2$-MgO.

1.2. Objectives

This study seeks to provide new understanding of the CaO-SiO_2-Al_2O_3-SO_3-$CaCl_2$-MgO system. Firstly, ye'elimite was targeted as the SO_3-containing phase, whereas alinite was targeted to accommodate $CaCl_2$ and MgO. The separate syntheses of ye'elimite and alinite are first investigated to understand their optimal process conditions for maximum formation. The ye'elemite and alinite produced were then blended in different amounts and fired to assess their co-existence. Then, the co-formation of ye'elemite and alinite in one-step sintering was investigated based on their overlapping formation conditions. The compatibility of alinite and ternesite is also tested and, finally, the co-formation of alinite and chlormayenite is studied with increasing contents of $CaCl_2$.

1.3. Clinker phases of interest

One clinker phase of interest in the system studied here is alinite, a structural variant of tricalcium silicate (alite) [9, 10]. This phase is interesting because it can incorporate chloride, magnesium and aluminium as shown in the chemical formula below, proposed by Neubauer et al. [9];

$$Ca_{10}\, Mg_{1-\frac{x}{2}}\, V_{\frac{x}{2}}\, [(SiO_4)_{3+x}\, (AlO_4)_{1-x}]\, O_2Cl \quad (1)$$

where the lattice vacancy (V) can be introduced depending on the substitution factor (x). Alinite cement was patented in the USSR in the 1970s and is reported to have been commercially produced by sintering raw materials at 1150°C [11]. Alinite cements are widely accepted to have comparable mechanical properties to Portland cement (PC) but with faster setting times [9, 12]. Table 1 compares the compositions of PC with that of alinite cements, C_3S, and with pure alinite produced at a substitution factor of 0.35 (x = 0.35) [9]. As shown in Table 1, significant amounts of chloride and MgO are included in alinite cements; thus, this clinker phase is a good candidate in the CaO-SiO_2-Al_2O_3-SO_3-$CaCl_2$-MgO system. The presence of chloride salt may also enhance the clinkering reactions by acting as a molten flux [13-16]. Ye'elimite ($C_4A_3\$$), which is the main phase in calcium sulfoaluminate based (CSA) cements, is another clinker phase of interest in the system studied. CSA cements require both a smaller amount of calcium component and a lower production temperature than PC [17]. Considering the compatible formation temperatures of alinite [9, 18] and ye'elimite [17], this study explores the feasibility of producing alinite-CSA clinker assemblages. Given the known compatibility issues of alite and ye'elimite under standard processing conditions [19], and the similar cementitious properties of alite and alinite [9, 12], the target clinker assemblage may provide an alternative to alite calcium sulfoaluminate (a-CSA) cements that may combine the favourable characteristics of PC and CSA cements [19]. Additionally, certain quantities of MgO in the raw meal have been found to improve the burnability

of raw meal and promote the formation of C_3S and $C_4A_3\$$ in a-CSA cements [20, 21].

Table 1. Oxide compositions (wt.%) of PC, alinite- based cements, and alinite (x=0.35) with general formula: $Ca_{10}Mg_{(1-x/2)}V_{(x/2)}[(SiO_4)_{(3+x)}(AlO_4)_{(1-x)}]O_2Cl$.

	PC [22]	Commercial alinite cement [11]	Other alinite cements [18, 23]	Pure alinite (x = 0.35) [9]	Stoichiometric alite (C_3S)
CaO	67	45 – 55	45 – 61	62	74
SiO_2	22	13 – 19	13 – 21	24	26
Al_2O_3	5	9 – 12	2 – 12	4	-
Fe_2O_3	3	4 – 10	2 – 10	-	-
MgO	<3	1 – 10	1 – 10	4	-
$CaCl_2$	-	6 – 18	4 – 18	6	-

2. Materials and methods

2.1. Materials

Raw mixtures were prepared from reagent grade chemicals: $CaCO_3$ (≥99%, Acros Organics), $CaSO_4$ (99%, Acros Organics), SiO_2 (99.5% Alfa Aesar), Al_2O_3 (≥99%, Acros Organics), $CaCl_2$ (96%, Acros Organics), and MgO (≥99.5%, Strem Chemicals Inc.).

2.2. Analysis techniques

X-ray diffraction (XRD) patterns were collected using a Panalytical X'Pert Pro PW3040 operating in reflection mode with Cu-Kα radiation (45 kV, 40

mA) and a diffracted beam monochromator (5.5 mm), at a scanning speed of 0.013° per second. All samples were backloaded, and measurements were conducted without rotation. Rietveld quantitative analysis was performed using Highscore plus (database PDF-4 2019) for all the samples, and the diffraction patterns used as a reference (Table 2) were from ICDD (International Centre for Diffraction Data) files.

Table 2. Phases detected in the products and the associated crystallographic information files/references used for Rietveld analysis.

Mineral name	Formula	Crystal system	Notation	ICCD PDF no.
Ye'elimite	$Ca_4(AlO_2)_6SO_3$	Orthorhombic	$C_4A_3\$$	01-083-9042 [24]
Mayenite	$Ca_{12}Al_{14}O_{33}$	Cubic	$C_{12}A_7$	01-073-6332 [25]
Krotite	$CaAl_2O_4$	Monoclinic	CA	01-077-3822 [26]
Corundum	Al_2O_3	Hexagonal	A	01-089-7716 [27]
Grossite	$CaAl_4O_7$	Monoclinic	CA_2	04-007-8974 [28]
Anhydrite	$CaSO_4$	Orthorhombic	C$	01-072-0916 [29]
Lime	CaO	Cubic	C	04-004-8985 [30]
Alinite	See Equation 1	Tetragonal	Alinite	04-012-3723 [31]
Chlormayenite	$Ca_{12}Al_{14}O_{32}Cl_2$	Cubic	$C_{11}A_7{\cdot}CaCl_2$	01-083-4322 [32]
Wadalite	$(Ca,Mg)_6(Al^{3+})_4((Si,Al)O_4)_3O_4Cl_3$	Isometric	Wadalite	04-017-5842 [33]
Larnite	Ca_2SiO_4	Monoclinic	β-C_2S	04-007-2687 [34]
Lime olivine	Ca_2SiO_4	Orthorhombic	γ-C_2Ss	04-010-9508 [34]
Ternesite	$Ca_5(SiO_4)_2SO_4$	Orthorhombic	$C_5S_2\$$	01-088-0812 [35]
Periclase	MgO	Isometric	M	04-003-5841 [36]
Hatrurite	Ca_3SiO_5	Trigonal	C_3S	00-049-0442 [34]
Chlorellestadite	$Ca_5(SiO_4)_{1.5}(SO_4)_{1.5}Cl$	Hexagonal	$3C_2S{\cdot}3C\$\cdot CaCl_2$	01-083-9122 [37]
Calcium chlorosilicate	$Ca_3SiO_4Cl_2$	Cubic	$C_2S{\cdot}CaCl_2$	04-013-7711 [38]

Apart from a good match between the measured and calculated Rietveld patterns, R_{wp} (weighted pattern residual error) and GOF (goodness of fit) values [39] below 10.0% and 5.0% respectively were required for reliable results [40]. To validate the Rietveld analysis, opportune calculations were performed; firstly, by retro-calculation from Rietveld quantification, the weight losses $\Delta wt.\%_{(R)}$ were obtained as a sum of CO_2 ($\Delta wt.\%CO_{2(R)}$), $CaCl_2$

(Δwt.%$CaCl_{2(R)}$) and SO_3 (Δwt.%$SO_{3(R)}$) losses; the difference between the experimental weight losses Δwt.%$_{(Exp)}$ and the calculated Δwt.%$_{(R)}$ was expressed as Δwt.%$_{(Exp-R)}$ and are reported in the Appendix. Furthermore, all the weight compositions were normalised only in terms of CaO (C), Al_2O_3 (A) and SiO_2 (S); the respective input/output differences ΔC, ΔA and ΔS (Appendix) would also allow for the evaluation of the Rietveld analysis. The lower the ΔC, ΔA, and ΔS values, the more reliable the solid phase quantification is. While MgO was not taken into account for this calculation because of its small content, both $CaCl_2$ and SO_3 were also excluded from this mass balance since they were volatile.

Simultaneous DSC/TG (SDT) analysis was performed on 20 – 40 mg of powder samples in a SDT Q600 (TA Instruments) instrument, operating between 50 °C and 1400 °C in an air atmosphere (flow rate 100 mL/min) at a heating rate of 10 °C / min; the samples were placed in disposable alumina crucibles for measurement.

2.3. Clinkering procedure

To ensure homogeneity, all the samples were prepared by blending the pre-dried powders for five minutes using a Rocklabs BenchTop Ring Mill (Scott products) within a Carbon/Chrome 100 head. Powders were then pelletised by applying a pressure of 11 atm; ~2 cm diameter and ~0.5 cm height pellets were obtained. All the pellets were placed in platinum crucibles and pre-

heated at 150°C for 30 minutes prior to firing. Preliminary experiments highlighted a lower efficiency in the synthesis of alinite when a ramp temperature program was used compared to when samples were inserted at target temperature; the gradual temperature increase led to increased volatilisation of $CaCl_2$. Since alinite was a main target phase, no ramp was used in clinkering. This method also enabled avoiding formation of any phases that are stable at a lower temperature, and that may then persist after heating; in this way, only phases stable at the target temperature will be observed. In all experiments, samples were fired once only at target temperature and only one sample was produced for each experiment using a consistent methodology.

All sintered products were cooled in air (fan-assisted) at room temperature before grinding and sieved below 75 µm for XRD analysis. The individual production of alinite was tested under different conditions aiming for a maximum conversion; two procedures were tested. The first method was based on the setup of Neubauer et al. [9] where the pellet was reacted in a sealed system. This was mimicked by using a sealed ceramic outer vessel with a total volume of 40 mL. The sealed system was provided with an extra source of $CaCl_2$, external to the sample, which was ~5 times the amount present in the reacting solid blend; this provided a $CaCl_2$-rich atmosphere within the system, inhibiting $CaCl_2$ escape from the raw-material mixture. In the second method, similar to that used by Vaidyanathan et al. [18], excess $CaCl_2$ was used directly within the raw-material mixture. Both studies [9, 18] indicated

optimal sintering conditions of 1150°C for 5 hours; in the present study, experiments were carried out at various temperatures and times as detailed in the following sections.

To investigate the possibility of single-stage manufacture of clinker containing both alinite and ye'elimite, the conditions allowing for the individual optimal production of each phase was tested. Variations in temperature and sintering time were investigated, and the conditions allowing for the maximum conversions were detected. Then, the phases produced from these tests were used as raw materials in a second stage of experiments, to study their co-existence upon re-firing. The co-formation of both alinite and ye'elimite was then attempted from raw-material mixtures. Finally, the production of clinkers mainly composed of alinite and chlormayenite was tested; the synthesis was characterised at different starting $CaCl_2$ contents in order to understand the effect of $CaCl_2$ content. It must be noted that no precautions were made for sulfur loss as it should not be significant below 1300°C where ye'elimite forms, and none of our experiments exceeded this temperature.

3. Results and discussion

3.1. Ye'elimite: synthesis optimisation

The starting solid mixture for $C_4A_3\$$ production was obtained by blending calcium carbonate (42.8 wt.%), aluminium oxide (39.6 wt.%), and calcium sulfate (17.6 wt.%) to allow for optimal yield [41]. The production of $C_4A_3\$$ was attempted by sintering the reactants for 1 or 2 hours at 1100°C, 1200°C, 1250°C, and 1300°C. Figure 1 shows the ye'elimite content detected within the samples produced; Rietveld analysis of the XRD data (Figure 2) enabled the quantification of the phases obtained (see SEI-I). No major differences were detected between the sintering times tested, whereas the operating temperature largely affected the formation of ye'elimite (Figure 1); a sharp increase was detected between 1200°C and 1250°C, from ~30 to 95 wt.%. A slight drop in ye'elimite content between 1250°C and 1300°C may be due to the onset of decomposition [42].

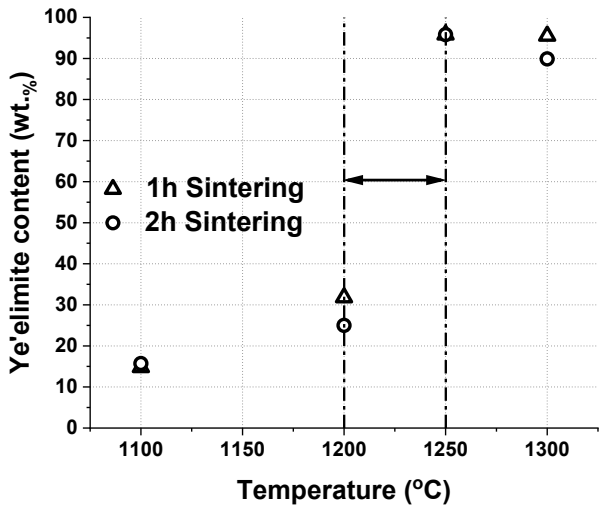

Fig. 1. $C_4A_3\$$ (wt.%) obtained through Rietveld analysis of samples Y_1 – Y_8. The trend shows a critical sintering zone above 1200°C and a favourable clinkering temperature of ye'elimite between 1250°C and 1300°C.

As shown in Figure 2, the decrease in the peak intensity of the reactants can be observed at higher temperatures, and their peaks were almost unidentifiable at 1250°C and 1300°C. Significant amounts of CA were identified at the lower temperatures and reduced at 1250°C and 1300°C, as the formation of ye'elimite was occurring at the expense of the calcium aluminate phases [43]. Furthermore, significant amounts of CA_2 were detected only at 1200°C. Low SO_3 losses were retro-calculated from Rietveld analysis of the samples within this series (see Appendix).

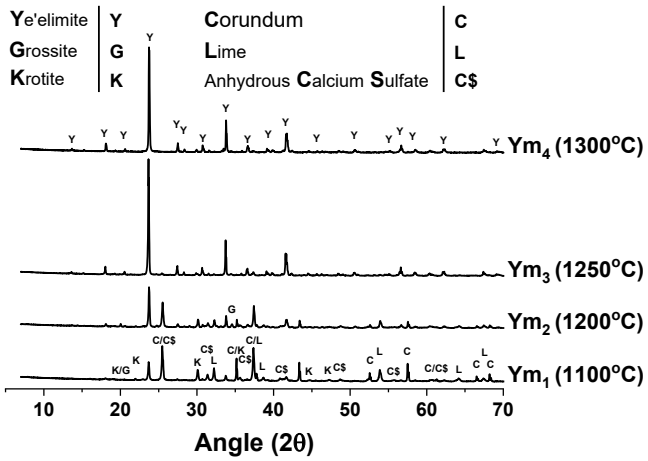

Fig. 2. Selected XRD patterns of ye'elimite synthesis samples, Y_1, Y_2, Y_3, and Y_4, sintered for 1 hour at 1100 °C, 1200 °C, 1250 °C, and 1300 °C respectively. Labels refer to the mineral name associated: Ye'elimite (Y), Grossite (G), Krotite (K), Corundum (C), Lime (L), Anhydrous Calcium Sulfate (C$).

3.2. Alinite: synthesis and optimisation

In order to assess the influence of the substitution factor x (in $Ca_{10}Mg_{1-x/2}V_{x/2}[(SiO_4)_{3+x}(AlO_4)_{1-x}]O_2Cl$) as well as the cooling rate, on alinite

formation, four samples were prepared by sintering at 1150°C for 5 hours [9]; the compositions used are shown in Table 3. Two samples were prepared at x = 0.35 for different cooling rates (N_1 and N_2), and two samples at x = 0.45 again for different cooling rates (N_3 and N_4). N_1 and N_3 were quenched at room temperature (fan-assisted), whereas N_2 and N_4 were kept sealed and slowly cooled down overnight within the muffle furnace by stopping the power input to the furnace after the desired sintering time.

Table 3. Raw mix and normalised (upon decarbonisation) batch oxide compositions (wt.%) for the alinite samples produced with substitution factors of x=0.35 and x=0.45 in $Ca_{10}Mg_{1-x/2}V_{x/2}[(SiO_4)_{3+x}(AlO_4)_{1-x}]O_2Cl$. Only the weight loss linked to the loss of CO_2 was considered for the normalisation.

		Raw-mix composition					Normalised composition				
x	Samples	Cc	S	$CaCl_2$	M	A	C	S	$CaCl_2$	M	A
0.35	**N_1-N_2**	74.6	15.8	4.4	2.6	2.6	62.2	23.5	6.5	3.9	3.9
0.45	**N_3-N_4**	74.7	16.3	4.4	2.4	2.2	62.4	24.2	6.5	3.6	3.3

Selected XRD patterns for samples in this series (N_1 and N_3) are shown in Figure 3; the main peak of alinite can be observed at 31.9° 2θ, and slightly lower intensities of alinite peaks could be observed for N_3 with respect to N_1, in accordance with the Rietveld XRD outcomes (see SEI-I). Furthermore, the production of small amounts of $C_2S{\cdot}CaCl_2$ could be observed for N_3, prepared with a substitution factor x = 0.45. By comparing the phase compositions of N_1 and N_3, a higher yield of alinite was observed at a substitution factor of 0.35 than 0.45, and the content of β-C_2S detected in N_3 was larger than in N_1. From N_1 and N_2, it is observed that quenching allows for a higher persistence of alinite. In the slow-cooled systems (N_2 and N_4), $C_2S{\cdot}CaCl_2$ was found as an

additional chlorine-containing phase. N_1 showed the highest production of alinite (72 wt.%), and therefore a substitution factor of 0.35 was considered here for the next set of experiments.

While small $\Delta CaCl_2(\%)_{(R)}$ values were observed for the quenched samples (N_1 and N_3), as shown in Appendix, negative values were calculated for N_2 and N_4. This suggests $CaCl_2$ uptake from the system atmosphere, provided by the external excess of $CaCl_2$, and leading to the overnight formation of $C_2S{\cdot}CaCl_2$. Nonetheless, the small differences in terms of ΔC, ΔA, and ΔS between the input and output oxides, suggest a good accuracy of the Rietveld analysis performed.

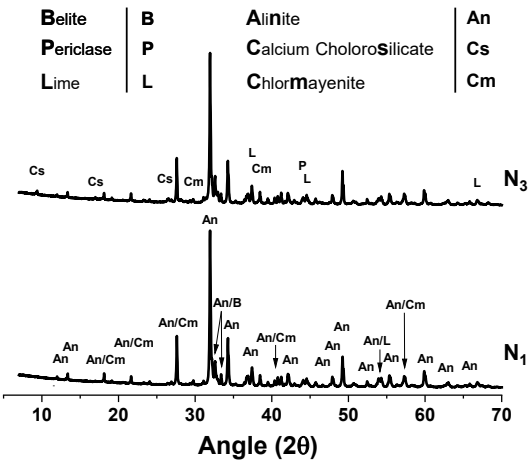

Fig. 3. XRD patterns of N_1 and N_3, yielding 72 and 64 wt.% alinite contents respectively. Labels refer to the mineral name associated: Alinite (An), Calcium Chlorosilicate (Cs), Chlormayenite (Cm), Belite (B), Periclase (P), Lime (L).

An alternative production method was also tested for alinite formation at x = 0.35 sintered at 1150°C for 5 hours, where excess $CaCl_2$ is directly added to

the raw mix batch [18], and the effects of cooling rate and sealing of the system were assessed. Samples P_1 and P_2 were sealed, P_3 and P_4 were not; P_1 and P_3 were quenched while P_2 and P_4 were slow-cooled; the $CaCl_2$ excess was 68 % (see SEI-I). In the sealed samples (P_1 and P_2), it is shown again that quenching (P_1) enhances the production of alinite, whereas slow cooling (P_2) led to the formation of $C_2S{\cdot}CaCl_2$. The higher yield of alinite in P_1 with respect to P_3 suggests that a sealed system also promotes the production of alinite, as observed in a parallel study [44], and this behaviour is related to a higher $CaCl_2$ partial pressure of the atmosphere surrounding the sample during the reaction, preventing the loss of chloride.

A difference in weight loss was recorded between sealed and unsealed samples after the heat treatment (33 wt.% and 35 wt.%, respectively), suggesting different amounts of $CaCl_2$ loss during heat treatment. This is confirmed by the lower $\Delta CaCl_{2(R)}$ values retro-calculated from Rietveld for the sealed samples P_1 and P_2 (see Appendix). Again, the formation of $C_2S{\cdot}CaCl_2$ in P_2 may have been enhanced by reaction with volatilised $CaCl_2$ still present in the sealed system during the overnight cooling within the furnace.

To optimise the manufacture of alinite alone, clinkering experiments were conducted at 1150°C, 1200°C, 1250°C, and 1300°C within a time range between 1 and 5 hours (An_1-An_{16} series), following the setup of experiment P_1; the Rietveld analyses are shown in SEI-I. As shown in Figure 4A, a higher temperature generally allows for a higher yield of alinite. The highest alinite contents were registered at 1300°C throughout the sintering times examined.

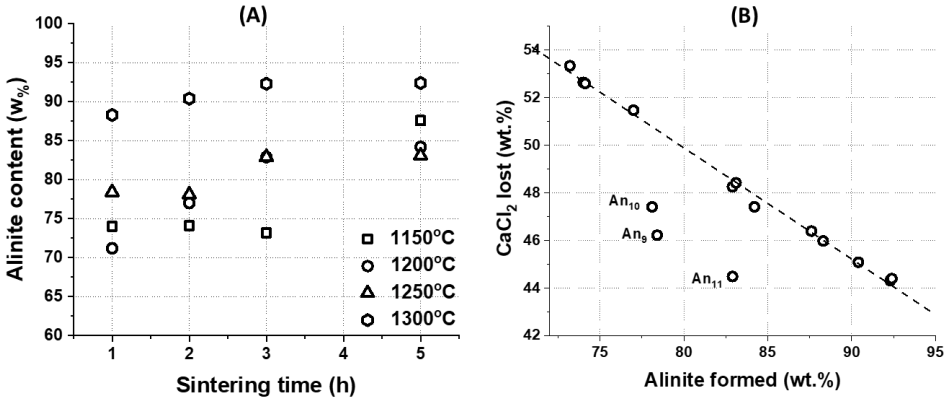

Fig. 4. Yield of alinite (x=0.35) obtained at four different clinkering temperatures with sintering times of 1, 2, 3, and 5 hours, corresponding to the samples An_1-An_{16} (Fig. 5A, left). $CaCl_2$ lost (wt.%) against the alinite percentage registered in the specific sample (Fig. 5B, right).

$CaCl_2$ losses were retro-calculated for all the samples presented in this experimental set. As shown in Figure 4B, a linear decreasing trend of $\Delta CaCl_2(\%)_{(R)}$ values was observed with increasing alinite contents. Slightly lower chloride loss was reported for those samples where $C_2S{\cdot}CaCl_2$ was produced (An_9, An_{10} and An_{11}).

3.3. Thermal analysis of alinite, ye'elimite and mixtures

Two of the batch mixtures used for the ye'elimite and alinite (P_n series) synthesis were subjected to thermal analysis, and the TG results are shown in Figure 5.

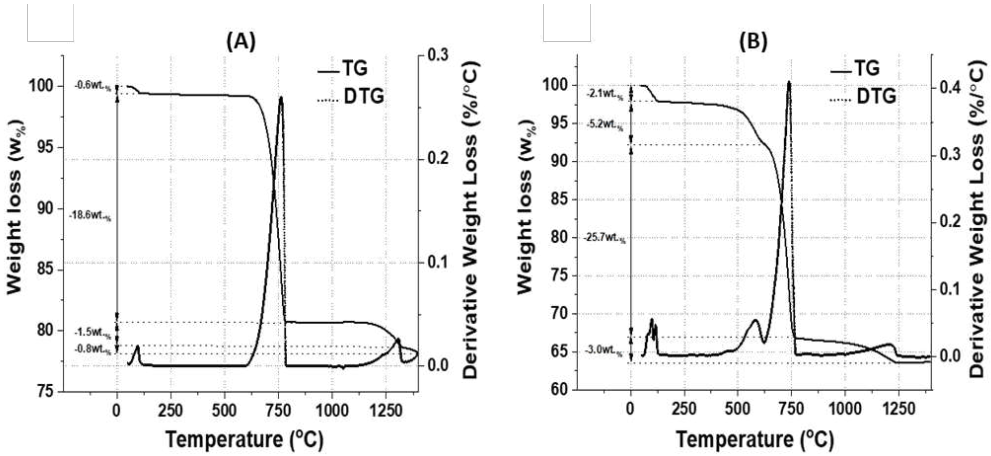

Fig.5. Weight loss (TG) and derivative weight loss (dTG) of raw mixtures used to synthesise ye'elimite (A) and alinite (B).

For the ye'elimite sample, the weight losses were observed in four temperature regions: ~100°C (0.6 wt.%), 600 – 800°C (18.6 wt. %), 1100 – 1350°C (1.5 wt.%) and 1350 - 1400°C (0.8 wt.%). They can be attributed to the dehydration of the hygroscopic calcium sulfate, carbon dioxide (from $CaCO_3$), SO_2 and O_2 from the thermal decomposition of calcium sulfate [45], and the beginning of ye'elimite decomposition [17], respectively.

For the alinite sample, the weight loss of 2.1 wt.% at around 100 °C is likely due to the dehydration of the hygroscopic calcium chloride, in addition to the water adsorbed on the raw powder reagents. A series of two overlapping main weight losses of 5.2 wt.% and 25.7 wt.% were detected within the temperature ranges 400 - 620°C and 620 - 800°C, respectively. Regarding the first temperature range, relative maximums could be observed at 405°C, 501°C and 595°C and they were probably linked to the evaporation of $CaCl_2$. $CaCl_2$ melts at 772°C, and Freidina et al. [46] reported the melting of the eutectic

303 $CaCl_2$ (70 mol%) - $CaCO_3$ (30 mol%) at 628°C and the eventual formation of
304 a double salt $CaCl_2 \cdot CaCO_3$. The proportioning of $CaCO_3$ (92 mol%) and
305 $CaCl_2$ (8 mol%) in the here-studied system would eventually lower the
306 melting and lead to the formation of intermediate $CaCl_2 \cdot CaCO_3$-based
307 compounds melting between 400°C and 620°C. Despite the partially masked
308 signal, a retro-calculated 52.0 wt.% $CaCl_2$ loss was calculated, in accordance
309 with the values registered for the P_n series (Figure 4B). Above 880°C, an
310 increasing weight loss of 3 wt.% with maximum at 1210°C is observed; this
311 may be attributed to weight loss from Cl-containing intermediate phases
312 eventually formed. A sharp endothermic peak at 1005°C in the DSC data
313 (SEI-II) is likely related to the formation of alinite [9].

314 The stoichiometric alinite/ye'elimite solid solutions at increasing weight
315 ratios 50:50, 70:30 and 80:20 (raw oxide batch compositions AY_1-AY_4, AY_5-
316 AY_6 and AY_7-AY_8 (see Table 6) were also tested by TG and DSC as shown
317 in Figure 6. Apart from the increasing water loss around 100°C, increasing
318 $CaCl_2$ initial contents led to higher weight losses in the temperature range
319 400°C - 620°C, confirming the link between $CaCl_2$ and the weight losses
320 observed in that temperature range in Figure 5. The presence of $CaSO_4$ may
321 have further contributed to the eutectic. The heat flows of mixtures are
322 reported in Figure 6B. No endothermic signal was detected at 1005°C,
323 previously linked to the formation of alinite, and suggesting that its formation
324 was inhibited.

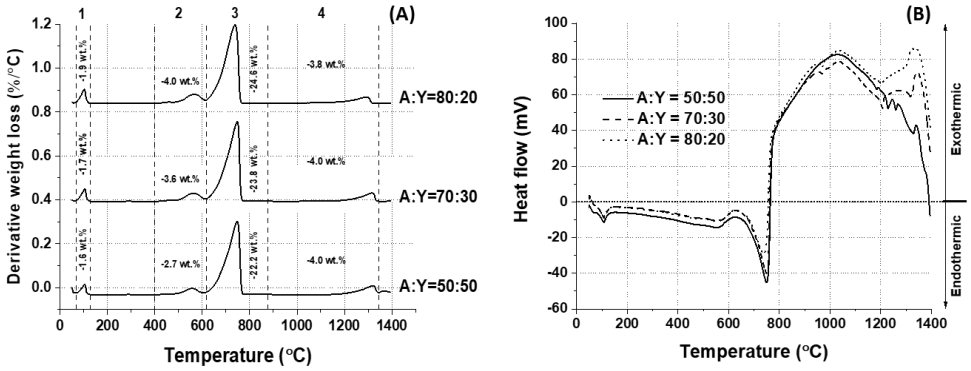

Fig.6. DTG (A) and heat flow (B) data for raw mixtures used to synthesise ye'elimite and alinite stoichiometric proportions of 50:50, 70:30 and 80:20 by weight.

3.4. Alinite and Ye'elimite: co-existence

To investigate the co-stability of alinite and ye'elimite, co-existence experiments were carried out. The first sintering procedure tested was to hold these synthetic phases at 1150°C for 5 hours, as this was found to be the best condition for alinite formation in the literature [9, 18]. Since pre-produced alinite and ye'elimite samples were used, the co-existence experiments were conducted in an open system (not sealed). To investigate the effects of a different proportioning of alinite and ye'elimite, two different compositions S_1a and S_2a (see table 4) were prepared according to a 50:50 (wt.%) blending of the pre-produced samples P_3-Y_{m2} and P_4-Y_{m3}, respectively. As a result, S_1a and S_2a represented the ye'elimite-poor and rich systems, respectively. The phases composition of the products S_1b and S_2b, obtained are also reported in Table 4. Although alinite was initially present as a main phase both in S_1a and

S_2a, no traces were detected after the sintering; chloride combined mainly as chlormayenite, and some wadalite.

Table 4. Phase composition (wt.%) of S_1 and S_2 before sintering (a), and the results of Rietveld analysis after sintering (b).

	Alinite	$C_4A_3\$$	$C_{11}A_7{\cdot}CaCl_2$	β-C_2S	C	CA_2	$C_5S_2\$$	CA	A	R_{wp}
S_1a	40	16	2	5	9	8	-	6	7	-
S_2a	41	48	2	5	2	-	-	-	-	-
S_1b	-	3	49	14	1	-	29	-	-	6.7
S_2b	-	10	46	15	1	-	27	-	-	7.1

***Sample S_1b also contained 2 wt.% of wadalite, samples S_1a, S_2a, S_1b and S_2b also contained 1, 2, 2 and 1 wt.% of M, respectively, sample S_1a also contained 7 wt.% of C$.**

Also, the amounts of ye'elimite and free lime dropped while larnite and chlormayenite increased. For both samples, Rietveld analysis over-estimated the chloride content, suggesting a slight uncertainty on the contents of the Cl-containing phases; slight $\Delta SO_{3(R)}$ values were also observed (see Appendix). The sulfur initially present in $C_4A_3\$$ and C$ appears to be combined as considerable quantities of ternesite ($C_5S_2\$$), which was not expected in the open system considered. In fact, ternesite formation is known to be enhanced in sealed or controlled systems that have a higher local partial pressure of SO_3 and O_2 [47-49]. Considering the improved hydraulic properties of ternesite produced in the presence of MgO [50] and its enhanced hydration in presence of mayenite [51], the clinker phase assemblages (containing ternesite and chlormayenite) produced in S_{1b} and S_{2b} are potentially interesting low-energy clinkers. The results presented in the previous sections showed improved alinite and ye'elimite formation at 1250 and 1300°C; therefore, these

temperatures were also tested to assess their co-existence at those conditions. Powder mixtures at different alinite/ye'elimite ratios were sintered for 60 minutes (not sealed) and then quenched to room temperature in air (fan-assisted). Three starting compositions were considered to produce the pairs of samples E_1-E_2, E_3-E_4 and E_5-E_6, respectively shown in Table 5. They were assembled by blending the pre-produced samples An_{16}-Y_{m7} 50:50 (wt.%), An_{16}-Y_{m3} 70:30 (wt.%) and An_{15}-Y_{m4} 80:20 (wt.%), respectively, and resulting in increasing alinite/ye'elimite ratios (see Table 5).

Table 5. Initial batch compositions of samples for alinite/ye'elimite co-existence experiments. E_1, E_3 and E_5 were sintered at 1300 °C while E_2, E_4 and E_6 at 1250 °C, for 60 mins.

Samples	Alinite	$C_4A_3\$$	$C_{11}A_7{\cdot}CaCl_2$	β-C_2S	Others*
E_1 and E_2	46	48	2	1	1
E_3 and E_4	65	29	1	4	-
E_5 and E_6	74	19	1	4	1

*** Others (<1 wt.%): C$, M, CA, sample E_5/E_6 also contained 1 wt.% of C, samples E_1/E_2 and E_3/E_4 also contained 2 and 1 wt% of $C_{12}A_7$, respectively.**

E_1, E_3 and E_5 were sintered at 1300°C while E_2, E_4 and E_6 at 1250°C. The outcomes from these experiments are all detailed in SEI-I, and they showed that alinite and ye'elimite could not co-exist in any of the systems studied; however, they reacted to form chlormayenite and belite and ternesite was not detected at these higher temperatures. Wadalite was identified in the most alinite-rich composition at 1300°C (E_5), while significant amounts of chlorellestadite and larnite were formed in the compositions with moderate to high proportions of alinite (E_3-E_6). No ye'elimite and reduced amounts of

alinite were observed in samples E_3 – E_6. In the more ye'elimite-rich system (E_1, E_2), sulfate ions tend to form calcium sulfate instead of chlorellestadite under these conditions, and small amounts of ye'elimite were still present.

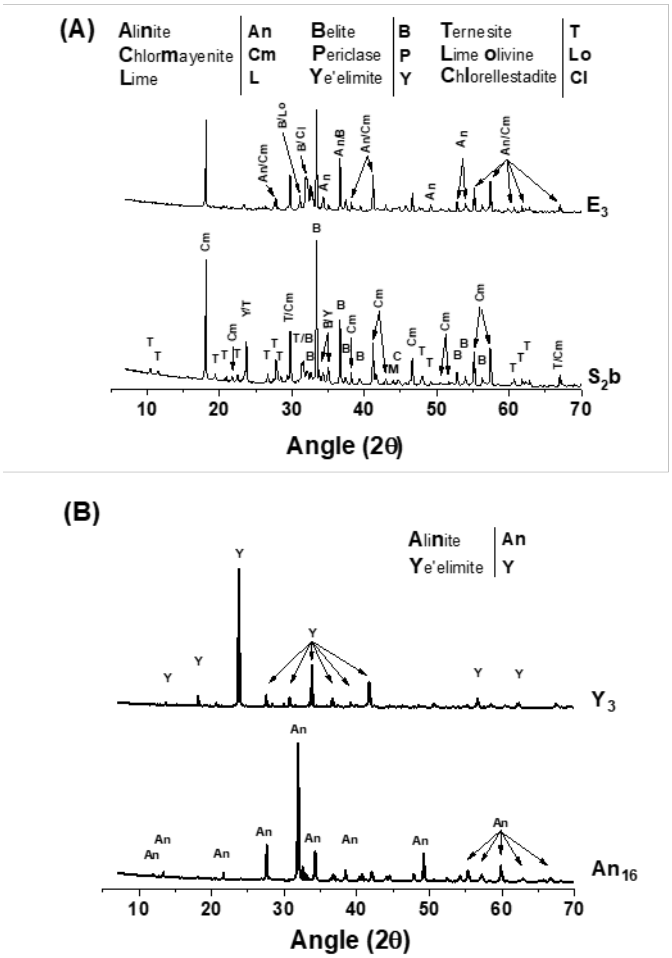

Fig. 7. Comparison between the XRD patterns of samples S_2 and E_3 (A, top) and An_{16} and Y_3 (B, bottom). Labels refer to the mineral name associated: Alinite (An), Chlormayenite (Cm), Lime (L), Belite (B), Periclase (P), Ye'elimite (Y), Ternesite (T), Lime olivine.

For all the E_1-E_6 samples, slightly negative $\Delta CaCl_2(\%)_{(R)}$ values were suggesting an over-estimation of the overall content in Cl-containing solid

395 phases detected; coupled with relatively high ΔC values (see Appendix), an
396 over-estimation of $C_{11}A_7{\cdot}CaCl_2$ is supposed. On the other hand, large
397 $\Delta SO_3(\%)_{(R)}$ values were suggesting a significant loss of $ from the solid
398 system for all the samples; in fact, a poor presence of SO_3-containing solid
399 phases was gained from Rietveld analysis, with no apparent dependence on
400 the sintering temperature. This suggests that the instability of ye'elimite in
401 these systems promoted the loss of sulfur from phases more volatile at these
402 temperatures. The XRD patterns of samples S_2b and E_3 (Figure 7A) show the
403 disappearance of both the alinite and ye'elimite phases pre-produced
404 separately (Figure 7B) and used in these experiments. The sample S_2b clearly
405 shows the formation of ternesite and its compatibility with chlormayenite at
406 1150°C.

407

408 ### *3.5. Co-formation experiments*

409

410 The co-formation of alinite and ye'elimite was tested using reagent grade
411 materials (see Table 5). As significant quantities of ternesite were found to
412 form in S_1b and S_2b, its compatibility with alinite was also assessed.
413 Additionally, as chlormayenite is the most compatible aluminate phase with
414 alinite, the possibility of co-producing them was tested along with the effect
415 of increasing $CaCl_2$ in the raw mix.

416

Table 6. Compositions (wt. %) of the raw mix, and normalised values accounting for decarbonisation.

Samples	Raw-mix composition						Normalised composition					
	Cc	**S**	**A**	**$CaCl_2$**	**C$**	**M**	**C**	**S**	**A**	**$CaCl_2$**	**C$**	**M**
$AY_1 – AY_4$	61.2	7.9	18.3	3.8	7.5	1.3	46.9	10.8	25.1	5.2	10.3	1.8
$AY_5 – AY_6$	65.6	10.9	11.9	5.3	4.5	1.8	51.7	15.3	16.7	7.4	6.3	2.5
$AY_7 – AY_8$	67.9	12.4	8.7	6.0	2.9	2.1	54.2	17.6	12.4	8.5	4.2	2.9
$AT_1 – AT_2$	66.8	16.8	1.3	3.8	10.0	1.3	53.1	23.8	1.8	5.5	14.2	1.8
AC_1	70.4	12.4	9.1	6.0	-	2.1	57.1	18.0	13.2	8.7	-	3.0
AC_2	69.6	12.4	9.4	6.5	-	2.0	56.2	17.9	13.6	9.4	-	2.9
AC_3	68.7	12.3	9.4	7.5	-	2.0	55.2	17.6	13.5	10.8	-	2.9
AC_4	68.1	12.2	9.2	8.5	-	2.0	54.5	17.4	13.1	12.2	-	2.8
AC_5	67.3	12.0	9.1	9.6	-	2.0	53.6	17.1	12.9	13.6	-	2.8

Samples AY_1-AY_4, AY_5-AY_6, and AY_7-AY_8 were designed for the stoichiometric formation of 50:50, 70:30, and 80:20 alinite:ye'elimite clinkers, respectively. Samples AT_1-AT_2 were prepared in order to obtain a stoichiometric 50:50 alinite:ternesite clinker. Samples AC_1-AC_5 were designed for the co-formation of a 80:20 alinite:chlormayenite clinker, which require 4.3 wt.% of Cl, but with higher and increasing quantities of excess (5.6, 6.0, 6.9, 7.8, and 8.7 wt.%) to assess the volatilisation of $CaCl_2$ during the sintering. AY_1 and AY_2 were first sintered at 1150°C for 3 and 5 hours respectively, to test the sintering parameters indicated by Neubauer et al. [9]. The optimal temperatures and clinkering time (1 hour) deduced in previous sections were also tested; specifically, AY_3, AY_5, and AY_7 were sintered at 1300°C, whereas AY_4, AY_6, and AY_8 at 1250°C. All the AY_n samples were sintered in a sealed system. The co-formation of alinite and ye'elimite was not observed at any condition tested; detailed phase compositions are provided in SEI-I. Regarding AY_1 and AY_2, no trace of alinite was detected but chlorine was found to preferably combine to form chlormayenite and/or

wadalite. Small amounts of ye'elimite were registered, but most of the sulfur component was found as ternesite, further promoting the interesting compatibility of ternesite with both belite and chlormayenite in the tested system. In accordance with the known behaviour of ternesite, which needs O_2 and SO_2 thermodynamic activity to form at higher temperatures [47], no ternesite was detected above 1150°C. In the samples AY_5-AY_8, higher overall contents of Cl, Mg, and Si allowed for enhanced alinite formation, but none of these samples contained $C_4A_3\$$. The formation of relevant amounts of C_3S was observed in both AY_5 and AY_7 at 1300°C, which in turn reduced the formation of β-C_2S and chlorellestadite compared with their counterparts sintered at 1250°C (AY_6 and AY_8, respectively). As an example, the XRD pattern of AY_7 is provided in Figure 8, where the characteristic peak of alite is observable at 14.9° 2θ. Alite is thermodynamically stable at 1250°C [52] but only practically forms at temperatures >1400°C [53], mineralisation by the presence of CaF_2 has been reported to reduce its formation temperature [54, 55], and similar mechanism may have occurred with chloride ions, as reported by Odler and Abdul-Maula [56] and Hanein et al. [16]; a low-temperature (around 1200°C) formation of C_3S was also observed by Chen et al. [57] using $CaCl_2$ and $CaSO_4$ as mineralizers for a more sustainable PC production.

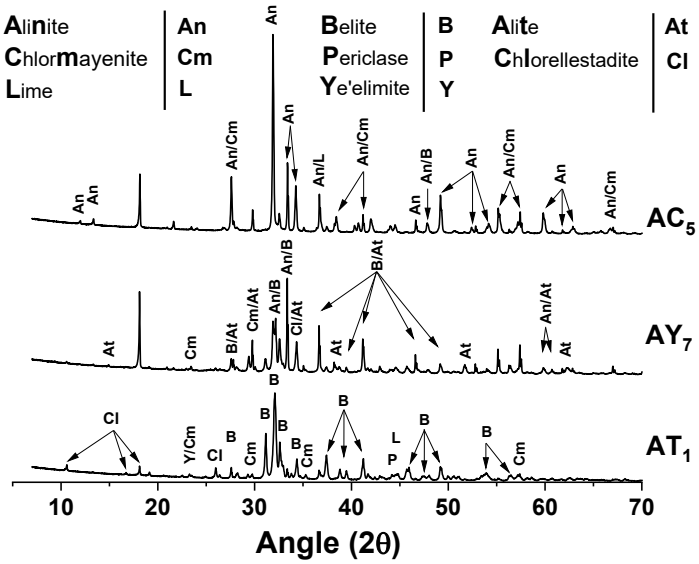

Fig. 8. XRD patterns of the samples AC_5, AY_7 and AT_1.

Significant amounts of chlormayenite were also found in all the AY_n samples, suggesting a weak dependence of its formation on sintering temperature in the range investigated, and small amounts of wadalite were also detected in all the samples. Regarding the samples AY_1-AY_4, higher $\Delta CaCl_2(\%)_{(R)}$ values of the samples sintered at 1150°C, compared to 1300°C (see Appendix), suggested combining of chloride within the solid mixture at higher temperatures. However, the higher $\Delta(\Delta wt.\%)_{(Exp-R)}$ values calculated for AY_3 and AY_4 might be linked to a greater $CaCl_2$ loss than that calculated from Rietveld analysis. On the other hand, the $\Delta SO_3(\%)_{(R)}$ values were suggesting a higher loss of SO_3 at 1300°C than 1150°C. Nonetheless, very low ΔC, ΔA, and ΔS values for all the AY_1-AY_4 samples suggest a good reliability of the Rietveld analysis performed here. Higher $CaCl_2$ losses were observed at

473 increasing initial $CaCl_2$ contents, in accordance with the TG analyses. On the
474 other hand, a significant difference in terms of SO_3 losses was observed
475 between the different compositions inspected; the negative $\Delta SO_3(\%)_{(R)}$ values
476 observed for AY_6 and AY_8 (see Appendix) suggest a slight over-estimation of
477 chlorellestadite and the relatively high ΔC and ΔA values for AY_6 and AY_8
478 confirm this assumption.

479 Samples AT_1 and AT_2 were sintered at 1150°C to test the co-formation of
480 alinite and ternesite. The samples were sealed and sintered for 3 (AT_1) and 5
481 (AT_2) hours. No significant differences were detected between products
482 sintered for 3 or 5 hours. β-C_2S was the main phase observed, accounting for
483 over the 50 wt.% in both samples. Only a small amount of alinite, one of the
484 target phases, was formed. The chlorine was incorporated mainly in
485 chlorellestadite (> 30 wt. %), and also small amounts in chlormayenite (< 4
486 wt.%). Ternesite, was not detected in these samples, suggesting that the co-
487 formation of alinite and ternesite is not possible under the processing
488 conditions used.

489 Finally, the co-formation of alinite and chlormayenite was tested with
490 increasing contents of excess $CaCl_2$ (samples AC_1-AC_5), as shown in Table
491 6. All the samples were sealed and sintered at 1300°C for 1 hour, then cooled
492 (fan-assisted) to room temperature; the detailed compositions are provided in
493 SEI-I. The amount of alinite formed increased with the initial $CaCl_2$ content
494 in the raw mix, ranging from ~63 wt.% to 74 wt. %; this is a very good
495 outcome, since the target based on raw mix stoichiometry was 80 wt.%. The

contents of chlormayenite were also close to the target of 20 wt.% in all samples and did not indicate any obvious trends related to the increase in $CaCl_2$ content in the raw-material mix. β-C_2S was also observed in decreasing quantities with increased quantities of initial $CaCl_2$. However, the amounts of minor phases such as β-C_2S and free lime are limited in AC_4 and AC_5 (< 5 wt.%); therefore the optimal excess of chlorine required to produce 80:20 alinite:chlormayenite by weight was 7.8–8.7 wt.% in the tested conditions. An overall weight loss of around 32 - 33 wt.% was observed for all these samples; the initial amount of calcium carbonate would contribute a 29 – 31 wt.% weight loss, suggesting that part of the $CaCl_2$ was also lost. The low ΔC, ΔA, ΔS values suggest a good reliability of the Rietveld analyses performed (see Appendix).

4. Implications for clinker manufacturing

The experiments conducted in this work demonstrate limited potential for the manufacture of ye'elimite - alinite clinkers in a single stage; these two phases were never found together in any sintered sample. Although some samples may not have fully reached equilibrium, a large portion of the results may be used to extend and validate thermodynamic studies [52] as well as open new areas of research to producing low-energy clinkers. This work will also spur interest in the use of chloride in cement manufacturing and the system studied

relates to various wastes which can be valorised for cement manufacture. Future work should study the inclusion of Fe_2O_3 in the evaluated clinker system.

In the context of clinker manufacture in a current industrial rotary kiln configuration, it must be noted that the kiln atmosphere, which is constantly renewed due to the counter-current operation, will have a constant composition varying at different parts of the process. This may inhibit or promote the formation or decomposition of volatile phases; for example, chloride may be lost at an earlier stage before reaching alinite formation temperature, as the raw meal is heating up and tumbling through the kiln. This, in turn, may also promote a volatilisation cycle and operational issues in existing kiln configurations.

5. Conclusions

Clinker assemblages in the system CaO-SiO_2-Al_2O_3-SO_3-$CaCl_2$-MgO have been produced and characterised. First, the individual production conditions of pure alinite and ye'elimite were optimised, and the optimal processing conditions observed for alinite contradict those declared in literature. More markedly, it is found that alinite and ye'elimite could not be simultaneously produced under any of the conditions tested. Co-existence experiments using pre-produced alinite-ye'elimite mixtures confirmed that these two phases are incompatible at clinkering temperatures. Furthermore, alinite and ternesite

could not be co-produced, also suggesting their incompatibility under the assessed processing conditions.

Alinite is compatible with both chlormayenite and belite; increasing $CaCl_2$ contents in the raw-material mix led to the formation of clinkers with higher alinite/belite ratios, while significant quantities of calcium chlorosilicate was detected in samples that were slow-cooled. Moreover, it is shown that in systems where ye'elimite is not stable, sulfur loss is more pronounced below 1300°C

The co-formation of ternesite and chlormayenite was observed and is attractive because of the low clinkering temperature of 1150°C. Also, the composition of the raw-material mix considered would lead to optimised hydraulic reactivity of ternesite. Chlorellestadite and wadalite are found to form at clinkering temperatures of the studied system and this offers a route to lock chloride in phases of lower hydraulic character when producing clinkers in this way. The formation of a significant amount of C_3S is observed after only 1 hour of sintering at 1300°C, suggesting that $CaCl_2$ can aid in the mineralisation of alite, and thus Portland cement systems. Moreover, the high compatibility observed between alinite and chlormayenite would suggest additional possibilities for the synthesis and testing of novel clinkers containing chloride. Consequently, this work uncovers new routes to improving resource efficiency and cement decarbonisation in a time where the world is seeking climate justice and pushing for an industrial circular economy.

APPENDIX. Summary of the ΔCO_2 (%), $\Delta CaCl_2$ (%) and ΔSO_3 (%) values retro-calculated from the Rietveld (R) analyses. The retro-calculated weight losses ($\Delta wt.\%_{(R)}$) are compared with the experimentally observed ones ($\Delta wt.\%_{(Exp)}$) and the difference) was reported in % as $\Delta(\Delta wt.\%)_{(Exp-R)}$. The normalised input/output differences referring to CaO, Al_2O_3 and SiO_2 (ΔC, ΔA and ΔS, respectively) are also reported.

ID	$\Delta CaCl_2$ (%) (R)	ΔSO_3 (%) (R)	ΔC	ΔA	ΔS	$\Delta wt.\%$ CO_2 (R)	$\Delta wt.\%$ $CaCl_2$ (R)	$\Delta wt.\%$ SO_3 (R)	Tot. $\Delta wt.\%$ (R)	$\Delta wt.\%$ (Exp)	$\Delta(\Delta wt.\%)$ (Exp-R)
Y_{m1}	-	2.6	1.1	-1.1	-	18.6	-	0.3	18.9	18.9	0.0
Y_{m2}	-	4.0	1.2	-1.2	-	18.6	-	0.4	19.0	19.5	0.5
Y_{m3}	-	1.2	1.1	-1.1	-	18.5	-	0.1	18.7	20.0	1.3
Y_{m4}	-	-3.0	0.9	-0.9	-	18.5	-	-0.3	18.2	19.7	1.5
Y_{m5}	-	-0.5	0.9	-0.9	-	18.5	-	-0.1	18.5	19.4	0.9
Y_{m6}	-	7.3	3.1	-3.1	-	18.1	-	0.8	18.9	19.6	0.7
Y_{m7}	-	1.2	1.2	-1.2	-	18.5	-	0.1	18.7	20.0	1.4
Y_{m8}	-	3.6	0.7	-0.7	-	18.7	-	0.4	19.1	20.3	1.1
N_1	22.4	-	0.7	-1.5	0.7	32.9	1.4	-	34.3	34.5	0.2
N_2	-54.4	-	1.5	-1.7	0.2	32.3	-3.5	-	28.8	32.7	3.9
N_3	17.3	-	1.2	-0.4	-0.8	32.8	1.1	-	34.0	33.2	-0.8
N_4	-10.3	-	1.1	-0.7	-0.4	32.7	-0.7	-	32.0	33.8	1.7
P_1	46.7	-	-0.3	-1.5	1.7	31.2	3.3	-	34.6	33.2	-1.4
P_2	26.9	-	-0.9	-1.0	1.9	30.8	1.9	-	32.8	33.7	1.0
P_3	50.2	-	-0.5	-1.2	1.7	31.4	3.6	-	34.9	34.7	-0.3
P_4	48.0	-	-0.9	-1.0	1.9	31.7	3.4	-	35.1	34.8	-0.3
An_1	53.5	-	0.7	-1.2	0.6	32.2	3.8	-	36.1	34.1	-2.0
An_2	53.3	-	0.6	-1.3	0.8	32.3	3.8	-	36.1	34.9	-1.2
An_3	54.0	-	0.4	-1.3	1.0	32.3	3.9	-	36.2	34.5	-1.6
An_4	46.3	-	0.5	-1.3	0.8	32.2	3.3	-	35.5	33.2	-2.3
An_5	51.7	-	0.6	-1.2	0.6	32.2	3.7	-	35.9	34.1	-1.8
An_6	51.7	-	0.6	-1.2	0.6	32.2	3.7	-	35.9	34.9	-1.1
An_7	48.5	-	0.5	-1.3	0.7	32.2	3.5	-	35.7	33.7	-2.0
An_8	47.6	-	0.6	-1.4	0.8	32.2	3.4	-	35.6	33.7	-1.9
An_9	46.4	-	0.9	-1.0	0.1	32.1	3.4	-	35.5	33.1	-2.4
An_{10}	47.6	-	0.9	-1.1	0.2	32.1	3.5	-	35.6	33.8	-1.8
An_{11}	44.7	-	0.7	-1.1	0.5	32.1	3.2	-	35.4	33.5	-1.9
An_{12}	48.7	-	0.4	-1.0	0.6	32.2	3.5	-	35.7	33.8	-1.9
An_{13}	46.2	-	0.8	-1.0	0.2	32.1	3.4	-	35.5	32.9	-2.5
An_{14}	45.3	-	0.7	-0.9	0.2	32.1	3.3	-	35.4	34.3	-1.1
An_{15}	44.5	-	0.5	-0.5	0.0	32.1	3.2	-	35.4	34.0	-1.4
An_{16}	45.4	-	0.4	-0.5	0.0	32.2	3.3	-	35.4	34.4	-1.1
S_1b	-32.9	12.1	1.9	-0.2	-1.7	-	-1.0	0.7	-0.2	0.5	0.7
S_2b	-22.4	5.4	3.2	-2.4	-0.8	-	-0.6	0.3	-0.3	0.4	0.7
E_1	-32.9	55.6	3.2	-3.1	-0.1	-	-1.6	3.4	-0.2	1.9	0.1
E_2	-22.4	71.4	2.7	-1.6	-1.1	-	-1.3	4.4	-0.3	2.1	-1.0
E_3	-19.3	42.7	3.5	-3.3	-0.2	-	-0.8	1.6	0.8	1.5	0.7
E_4	-21.0	45.2	3.3	-3.0	-0.3	-	-0.9	1.7	0.9	1.1	0.2
E_5	-14.9	77.9	1.0	1.0	-1.9	-	-0.7	2.1	1.4	2.3	0.9
E_6	-24.7	77.6	2.0	-1.9	-0.1	-	-1.2	2.1	0.9	1.2	0.3
AT_1	21.7	6.5	1.3	-0.3	-1.0	29.6	0.8	0.4	30.8	31.3	0.4
AT_2	20.3	6.8	1.3	-0.3	-1.0	29.6	0.8	0.4	30.8	31.5	0.7
AY_1	31.3	9.1	0.8	-1.2	0.4	26.1	1.2	0.4	27.7	27.5	-0.2
AY_2	38.4	4.6	1.0	-1.6	0.6	26.0	1.5	0.2	27.8	27.4	-0.4
AY_3	17.3	78.9	1.0	-2.2	1.2	26.9	0.6	3.4	30.9	27.3	-3.6
AY_4	17.3	83.7	0.8	-2.2	1.4	27.0	0.6	3.6	31.2	27.3	-3.9
AY_5	38.3	15.2	2.2	-2.8	0.6	28.5	2.0	0.4	30.9	29.3	-1.6
AY_6	32.2	-13.8	3.1	-3.2	0.1	28.1	1.8	-0.4	29.5	29.3	-0.2
AY_7	50.5	10.6	1.4	-0.5	-0.9	30.1	3.0	0.2	33.2	30.7	-2.5
AY_8	47.5	-22.6	3.1	-3.0	-0.2	29.4	2.9	-0.4	31.9	30.8	-1.1
AC_1	31.1	-	1.1	-0.9	-0.2	31.1	1.8	-	32.9	32.3	-0.6
AC_2	32.7	-	0.5	-0.8	0.3	30.9	2.1	-	32.9	32.9	0.0
AC_3	41.4	-	0.8	-1.9	1.1	30.6	3.0	-	33.6	32.6	-1.0
AC_4	46.9	-	0.4	-1.7	1.3	30.5	3.8	-	34.3	32.6	-1.7
AC_5	51.4	-	-0.4	0.1	0.3	30.4	4.6	-	35.0	32.1	-2.9

Acknowledgements

This work was funded by the Dr Jeff Wadsworth – Battelle Visiting Research Fellowship (2019) awarded by the University of Sheffield (R/156208-20-1) and undertaken at the University of Kentucky Centre for Applied Energy Research (UK-CAER). The authors would like to thank Anne E. Oberlink, John Wiseman, and Thomas L. Robl for their support. This work was also supported by the Engineering and Physical Science Research Council (EPSRC) through grant: EP/R025959/1.

Table of Figures

Fig. 1. *$C_4A_3\$$ (wt.%) obtained through Rietveld analysis of samples Y_1 – Y_8. The trend shows a critical sintering zone above 1200°C and a favourable clinkering temperature of ye'elimite between 1250°C and 1300°C.*

Fig. 2. *Selected XRD patterns of ye'elimite synthesis samples, Y_1, Y_2, Y_3, and Y_4, sintered for 1 hour at 1100 °C, 1200 °C, 1250 °C, and 1300 °C respectively. Labels refer to the mineral name associated: Ye'elimite (Y), Grossite (G), Krotite (K), Corundum (C), Lime (L), Anhydrous Calcium Sulfate (C$).*

Fig.3. *XRD patterns of N_1 and N_3, yielding 72 and 64 wt.% alinite contents respectively. Labels refer to the mineral name associated: Alinite (An), Calcium Chlorosilicate (Cs), Chlormayenite (Cm), Belite (B), Periclase (P), Lime (L).*

Fig.4. *Yield of alinite (x=0.35) obtained at four different clinkering temperatures with sintering times of 1, 2, 3, and 5 hours, corresponding to the samples An_1-An_{16} (Fig. 5A, left). $CaCl_2$ lost (wt.%) against the alinite percentage registered in the specific sample (Fig. 5B, right).*

Fig.5. *Weight loss (TG) and derivative weight loss (dTG) of raw mixtures used to synthesise ye'elimite (A) and alinite (B).*

Fig.6. *DTG (A) and heat flow (B) data for raw mixtures used to synthesise ye'elimite and alinite stoichiometric proportions of 50:50, 70:30 and 80:20 by weight.*

Fig.7 *Comparison between the XRD patterns of samples S_2 and E_3 (A, top) and An_{16} and Y_3 (B, bottom). Labels refer to the mineral name associated: Alinite (An), Chlormayenite (Cm), Lime (L), Belite (B), Periclase (P), Ye'elimite (Y), Ternesite (T), Lime olivine.*

Fig.8. XRD patterns of the samples AC_5, AY_7 and AT_1.

References

1. Olivier, J.G.J., et al., *Trends in global CO_2 emissions: 2016 Report*. 2016, PBL Netherlands Environmental Assessment Agency Hague and European Commission Joint Research Centre Institute for Environment and Sustainability.
2. Polettini, A., et al., *Properties of Portland cement—stabilised MSWI fly ashes.* Journal of Hazardous Materials, 2001. **88**(1): p. 123-138.
3. Yan, D.Y.S., et al., *Development of controlled low-strength material derived from beneficial reuse of bottom ash and sediment for green construction.* Construction and Building Materials, 2014. **64**: p. 201-207.
4. Yang, J.E., et al., *Reclamation of abandoned coal mine waste in Korea using lime cake by-products.* Mine Water and the Environment, 2006. **25**(4): p. 227-232.
5. Sorell, G., *The role of chlorine in high temperature corrosion in waste-to-energy plants.* Materials at high temperatures, 1997. **14**(3): p. 207-220.
6. Hans, S., *Production of soda ash*. 1958, Google Patents.
7. Du, R.-g., et al., *Effect of chlorine ions on the corrosion behavior of reinforcing steel in concrete [J].* Materials Protection, 2006. **6**.
8. Scrivener, K.L., et al., *Eco-efficient cements: Potential economically viable solutions for a low-CO_2 cement-based materials industry.* Cement and Concrete Research, 2018. **114**: p. 2-26.
9. Neubauer, J., and Pöllmann, H., *Alinite—Chemical composition, solid solution and hydration behaviour.* Cement and concrete research, 1994. **24**(8): p. 1413-1422.
10. Ilyukhin, V.V., et al., *Crystal structure of alinite.* Nature, 1977. **269**(5627): p. 397-398.
11. Hewlett, P., *Lea's chemistry of cement and concrete*. 4th ed. 1998: London: Edward Arnold.
12. Uçal, G.O., et al., *Hydration of alinite cement produced from soda waste sludge.* Construction and Building Materials, 2018. **164**: p. 178-184.
13. Photiadis, G., et al., *Low energy synthesis of cement compounds in molten salt.* Advances in Applied Ceramics, 2011. **110**(3): p. 137-141.
14. Hanein, T., et al., *Prospects for manufacturing cement compounds in molten salt fluxed systems.* Prospects, 2017. **11**: p. 12.
15. Hanein, T., et al. *Molten salt synthesis of compounds related to cement, 1st International Conference on Cement and Concrete Technology, Muscat, Oman. 2017*.
16. Hanein, T., et al., *Pyro processing cement kiln bypass dust: Enhancing clinker phase formation.* Construction and Building Materials, 2020. **259**: p. 120420.
17. Hanein, T., et al., *Carbon footprint of calcium sulfoaluminate clinker production.* Journal of Cleaner Production, 2018. **172**: p. 2278-2287.
18. Vaidyanathan, D., et al., *Production and properties of alinite cements from steel plant wastes.* Cement and Concrete Research, 1990. **20**(1): p. 15-24.
19. Hanein, T., et al., *Alite calcium sulfoaluminate cement: chemistry and thermodynamics.* Advances in Cement Research, 2019. **31**(3): p. 94-105.
20. Liu, X., and Li, Y., *Effect of MgO on the composition and properties of alite-sulphoaluminate cement.* Cement and concrete research, 2005. **35**(9): p. 1685-1687.
21. Liu, X., et al., *Influence of MgO on the formation of Ca_3SiO_5 and $3CaO\cdot 3Al_2O_3\cdot CaSO_4$ minerals in alite–sulphoaluminate cement.* Cement and Concrete Research, 2002. **32**(7): p. 1125-1129.
22. Taylor, H.F.W., *Cement chemistry.* Telford, London, 1997.
23. Kapur, P., and Kapur, P.C., *Manufacture of eco-friendly and energy-efficient alinite cements from flyashes and other bulk wastes.* Resources Processing, 2004. **51**(1): p. 8-13.
24. Cuesta, A., et al., *Structure, atomistic simulations, and phase transition of stoichiometric yeelimite.* Chemistry of Materials, 2013. **25**(9): p. 1680-1687.
25. Büssem, W., *Die Struktur des Pentacalciumtrialuminats.* Zeitschrift für Kristallographie-Crystalline Materials, 1936. **95**(1-6): p. 175-188.

26. Palacios, L., et al., *Crystal structures and in-situ formation study of mayenite electrides.* Inorganic chemistry, 2007. **46**(10): p. 4167-4176.
27. Oetzel, M. and G. Heger, *Laboratory X-ray powder diffraction: a comparison of different geometries with special attention to the usage of the Cu Kα doublet.* Journal of Applied Crystallography, 1999. **32**(4): p. 799-807.
28. Goodwin, D.W. and A.J. Lindop, *The crystal structure of $CaO.2Al_2O_3$.* Acta Crystallographica Section B: Structural Crystallography and Crystal Chemistry, 1970. **26**(9): p. 1230-1235.
29. Kirfel, A. and G. Will, *Charge density in anhydrite, $CaSO_4$, from X-ray and neutron diffraction measurements.* Acta Crystallographica Section B: Structural Crystallography and Crystal Chemistry, 1980. **36**(12): p. 2881-2890.
30. Taylor, D., *The structural behaviour of tetrahedral framework compounds—a review Part II. Framework structures.* Mineralogical Magazine, 1984. **48**(346): p. 65-79.
31. Il'inets, A.M. and M. Bikbau, *Peculiarities of the atomic structure of alinite and jasmundite.* Kristallografiya, 1989. **34**(1): p. 71-7.
32. Schmidt, A., et al., *Chlorine ion mobility in Cl-mayenite ($Ca_{12}Al_{14}O_{32}Cl_2$): An investigation combining high-temperature neutron powder diffraction, impedance spectroscopy and quantum-chemical calculations.* Solid State Ionics, 2014. **254**: p. 48-58.
33. Gobechiya, E.R., et al., *Calcio-olivine γ-Ca_2SiO_4: I. Rietveld refinement of the crystal structure.* Crystallography Reports, 2008. **53**(3): p. 404-408.
34. Mumme, W.G., et al., *Rietveld crystal structure refinements, crystal chemistry and calculated powder diffraction data for the polymorphs of dicalcium silicate and related phases.* 1995.
35. Irran, E., et al., *Ternesite, $Ca_5(SiO_4)_2SO_4$, a new mineral from the Ettringer Bellerberg/Eifel, Germany.* Mineralogy and Petrology, 1997. **60**(1-2): p. 121-132.
36. Goldschmidt, V.M., et al., *Geochemical distribution law of the elements. VII. Summary of the chemistry of crystals.* Skr. Nor. Vidensk. Akad, 1926. **1**: p. 1-117.
37. Fang, Y.N., et al., *Crystal chemical characteristics of ellestadite-type apatite: implications for toxic metal immobilization.* Dalton Transactions, 2014. **43**(42): p. 16031-16043.
38. Czaya, R. and Bissert, G., *Die Kristallstruktur von Tricalciummonosilikatdichlorid ($Ca_2SiO_4.CaCl_2$).* Acta Crystallographica Section B: Structural Crystallography and Crystal Chemistry, 1971. **27**(4): p. 747-752.
39. Toby, B.H., *R factors in Rietveld analysis: How good is good enough?* Powder diffraction, 2006. **21**(1): p. 67-70.
40. Young, R.A., *The rietveld method*. Vol. 5. 1993: International union of crystallography.
41. Simoni, M., et al., *On cement clinker assemblages containing alinite, calcium sulfoaluminate and calcium aluminates*. in *Low Carbon Conference 3 (LOWC3) 2020*. 2020. Lexington.
42. Hanein, T., et al. *Thermodynamic data of ye'elemite (C_4A_3S) for cement clinker equilibrium calculations*. in *35th Cement & Concrete Science Conference.* 2015. Aberdeen.
43. El Khessaimi, Y., et al., *Solid-state synthesis of pure ye'elimite.* Journal of the European Ceramic Society, 2018. **38**(9): p. 3401-3411.
44. Simoni, M., et al. *Continuous production of alinite in a laboratory-scale rotary kiln*. in *74th RILEM Annual Week and 40th Cement and Concrete Science Conference*. 2020. Sheffield.
45. Fukami, T., et al., *Synthesis, Crystal Structure, and Thermal Properties of $CaSO_4*2H_2O$ Single Crystals.* International journal of chemistry, 2015. **15**(2): p. 12-20.
46. Freidina, E.B. and Fray, D.J., *Phase diagram of the system $CaCl_2$–$CaCO_3$.* Thermochimica acta, 2000. **351**(1-2): p. 107-108.
47. Hanein, T., et al., *Stability of ternesite and the production at scale of ternesite-based clinkers.* Cement and Concrete Research, 2017. **98**(C): p. 91-100
48. Galan, I., et al., *Advances in clinkering technology of calcium sulfoaluminate cement.* Advances in Cement Research, 2017.
49. Galan, I., et al., *Phase Compatibility in the System CaO–SiO_2–Al_2O_3–SO_3–Fe_2O_3 and the Effect of Partial Pressure on the Phase Stability.* Industrial & Engineering Chemistry Research, 2017. **56**(9): p. 2341-2349.
50. Skalamprinos, S., et al., *The synthesis and hydration of ternesite, $Ca_5(SiO_4)_2SO_4$.* Cement and Concrete Research, 2018. **113**: p. 27-40.

51. Montes, M., et al., *Can calcium aluminates activate ternesite hydration?* Cement and Concrete Research, 2018. **103**: p. 204-215.
52. Hanein, T., et al., *Thermodynamic data for cement clinkering.* Cement and Concrete Research, 2020. **132**: p. 106043.
53. Taylor, H.F.W., *Cement chemistry. 2nd* ed., T Telford, London, 459pp, 1997.
54. Dominguez, O., et al., *Characterization using thermomechanical and differential thermal analysis of the sinterization of Portland clinker doped with CaF_2.* Materials characterization, 2010. **61**(4): p. 459-466.
55. Shame, E.G., and Glasser, F.P., *Stable Ca_3SiO_5 solid solutions containing fluorine and aluminium made between 1050°C and 1250° C.* British ceramic. Transactions and journal, 1987. **86**(1): p. 13-17.
56. Odler, I. and Abdul-Maula, S., *Effect of mineralizers on the burning of portland cement clinker: I, Kinetics of the process.* ZKG, Zement-Kalk-Gips, Edition A, 1980. **33**: p. 132-6.
57. Chen, M., and Fang, Y., *The chemical composition and crystal parameters of calcium chlorosulfatosilicate.* Cement and Concrete Research, 1989. **19**(2): p. 184-188.